

Effect of Shearing Laminar Flow on Dielectric Polarization of Suspensions of Rigid Particles

B. George Barisas¹

Department of Chemistry, Yale University, New Haven, Connecticut 06520.
Received October 9, 1973

ABSTRACT: Application of shear to a solution of macromolecules undergoing dielectric measurements can cause a variation in the measured polarization of the solute. The theories of Saito and Kato and of Peterlin and Reinhold treat this phenomenon for rigid and flexible macromolecules, respectively, where both the velocity gradients and electric fields applied to the solutions are small. In this study the former model has been extended to apply to the case of large velocity gradients and time-independent electric and shear fields. The ratio of the polarization observed at a velocity gradient g to the polarization at zero velocity gradient is calculated and tabulated for various axial ratios of prolate and oblate ellipsoids and for values of g ranging from 0 to $100D$ where D is the rotary diffusion constant of the particle. For all axial ratios of ellipsoids a decrease in this ratio with increasing shear is predicted. The results are compared with a closed form expression derivable for the case of a sphere.

The effect of shearing laminar flow on the measured dielectric constant of dilute solutions of macromolecules has been the subject of at least two theoretical studies. Saito and Kato^{2a} considered rigid ellipsoids of rotation possessing a permanent dipole moment along the symmetry axis. When the direction of fluid flow was taken perpendicular to the applied electric field, a decrease in dielectric polarization with the square of the velocity gradient was predicted. Peterlin and Reinhold^{2b} have examined the case of a necklace of beads joined by perfectly elastic links. Where monomer dipoles are directed parallel to the chain, no shear dependence of the polarization is predicted, while for monomer dipoles perpendicular to the chain, the polarization increases with the square of velocity gradient. Experimental verification of these models has been limited. A study by Wendisch³ of randomly coiled cellulose nitrate supports the predictions of Peterlin and Reinhold for flexible polymers. Similarly experiments on DNA⁴ and on helical poly(γ -benzyl L-glutamate) (PBLG)^{5,6} have shown that the orientation polarization of these polymers decreases when shearing stresses sufficient to cause non-Newtonian viscosity effects are applied to these solutions in a direction perpendicular to the electric field. Since no model was available to predict quantitatively these effects at large velocity gradients, the theory of Saito and Kato was reexamined with a view to extending its application to these experimental situations.

Three major modifications were made in their treatment of the problem so that it might relate more directly to experimental data. First, the distribution function of Saito and Kato is based on a power series in the velocity gradient and electric field. As will be shown later, the expression for dielectric polarization based on this series does not con-

Further, dielectric measurements are frequently extrapolated to zero frequency. Thus the model may be greatly simplified by assuming time-independent values of both applied fields. Third, electric fields employed in dielectric measurements are rarely sufficient to cause electric saturation of the sample. Thus the polarization may be calculated by retaining only first-order effects of the electric field on the distribution function determined by hydrodynamic forces.

Thus modified the treatment of Saito and Kato has been developed to yield values of the ratio of the polarization observed at a velocity gradient g to the polarization at zero velocity gradient for values of g ranging from zero to $100D$ where D is the rotary diffusion constant of the particle. For all shapes of ellipsoids of revolution, a decrease in this ratio with increasing shear is predicted. This agrees with a trivial closed form solution which obtains for a spherical particle.

Theory

The reader is referred to the work of Saito and Kato^{2a} for a detailed description of the model employed. The electric field E is in the x direction while the fluid flow is along the y axis with velocity gradient g along the x axis. The distribution function F is given by the diffusion equation

$$\nabla(D\nabla F - F\bar{\omega}) = \partial F / \partial t \quad (1)$$

where D is the rotary diffusion constant of the particle and $\bar{\omega}$ is its angular velocity due to hydrodynamic and electric forces. Setting $\gamma = g/2D$ and $\epsilon = \mu E/kT$ and expanding $\bar{\omega}$, one obtains

$$\nabla^2 F - \left\{ \begin{array}{ll} [\gamma(1 + p \cos 2\phi)] & + \epsilon(-\sin \phi / \sin \theta) \frac{\partial F}{\partial \phi} \\ + [\gamma(p \sin \theta \cos \theta \sin 2\phi)] & + \epsilon(\cos \theta \cos \phi) \frac{\partial F}{\partial \theta} \\ + [\gamma(-3p \sin^2 \theta \cos 2\phi)] & + \epsilon(-2 \sin \theta \cos \phi) F \end{array} \right\} = \frac{1}{D} \frac{\partial F}{\partial t} \quad (2)$$

verge for large values of the velocity gradient. A different approach is necessary to calculate the polarization at realistically large values of applied shear. Second, these workers assumed sinusoidal oscillation of the applied fields and considerable complexity in calculation resulted. Dielectric measurements on a solution undergoing shear are most easily performed using a Couette-type apparatus and such instruments customarily operate at constant angular velocity.

where $p = (r^2 - 1)/(r^2 + 1)$ is a function of the axial ratio r of the particle. Consideration can generally be restricted to the case where both the shear and electric fields are time invariant. It is possible to write F as a power series in γ and ϵ

$$F = \sum_{ij} \gamma^i \epsilon^j F_{ij} \quad (3)$$

where each F_{ij} is a sum of spherical harmonics.

Table I
 $\langle \mu \rangle_g / \langle \mu \rangle_0$ as a Function of $g/2D$ and Axial Ratio

$g/2D$	Axial ratio												
	∞	50	20	10	5	2	1	0.5	0.2	0.1	0.05	0.02	0
0	1.000	1.000	1.000	1.000	1.000	1.000	1.000	1.000	1.000	1.000	1.000	1.000	1.000
0.1	0.998	0.998	0.998	0.998	0.998	0.998	0.998	0.997	0.997	0.997	0.997	0.997	0.997
0.14	0.997	0.997	0.997	0.997	0.997	0.996	0.995	0.994	0.994	0.994	0.994	0.994	0.994
0.2	0.994	0.994	0.994	0.994	0.993	0.992	0.990	0.988	0.987	0.987	0.987	0.987	0.987
0.3	0.986	0.986	0.986	0.986	0.985	0.983	0.978	0.974	0.972	0.972	0.972	0.972	0.972
0.4	0.976	0.976	0.976	0.976	0.975	0.970	0.962	0.955	0.951	0.951	0.951	0.951	0.951
0.5	0.963	0.963	0.963	0.963	0.961	0.954	0.941	0.931	0.926	0.925	0.925	0.925	0.925
0.7	0.932	0.932	0.931	0.931	0.928	0.914	0.891	0.873	0.865	0.864	0.863	0.863	0.863
1.0	0.875	0.875	0.874	0.873	0.868	0.842	0.800	0.770	0.759	0.757	0.757	0.757	0.757
1.4	0.793	0.793	0.793	0.790	0.782	0.737	0.671	0.630	0.619	0.618	0.617	0.617	0.617
2	0.683	0.683	0.681	0.678	0.664	0.594	0.500	0.456	0.451	0.452	0.452	0.452	0.452
3	0.547	0.547	0.545	0.540	0.519	0.420	0.308	0.275	0.286	0.289	0.291	0.291	0.291
5	0.396	0.395	0.393	0.386	0.358	0.237	0.138	0.128	0.151	0.157	0.159	0.159	0.160
7	0.316	0.315	0.313	0.304	0.272	0.152	0.075	0.073	0.097	0.104	0.106	0.107	0.107
10	0.247	0.246	0.243	0.234	0.200	0.090	0.038	0.039	0.060	0.067	0.069	0.069	0.070
14	0.195	0.195	0.192	0.181	0.147	0.052	0.020	0.021	0.038	0.044	0.046	0.046	0.046
20	0.152	0.151	0.148	0.137	0.103	0.028	0.010	0.011	0.022	0.028	0.029	0.030	0.030
30	0.119	0.118	0.114	0.102	0.068	0.013	0.004	0.005	0.012	0.016	0.018	0.018	0.018
50	0.082	0.081	0.077	0.066	0.037	0.005	0.002	0.002	0.005	0.008	0.010	0.010	0.010

$$F_{ij} = \frac{1}{4\pi} \sum_{n=0}^{2i+j} \sum_{m=0}^n P_n^m(\cos \theta) [{}_{ij}a_n^m \cos m\phi + {}_{ij}b_n^m \sin m\phi] \quad (4)$$

The induced dipole moment at shear rate g , $\langle \mu \rangle_g$, is simply the component of the dipole moment along the electric field direction averaged with respect to this distribution function.

$$\langle \mu \rangle_g = \mu \iint F \sin^2 \theta \cos \phi \, d\theta d\phi \quad (5)$$

If only the terms first order in the electric field are retained

$$\begin{aligned} \langle \mu \rangle_g &= -\frac{\mu \epsilon}{3} \sum_{i=0}^{\infty} {}_{i1}a_1^1 \gamma^{2i} \\ &= -\frac{\mu \epsilon}{3} \left[-1 + \left(\frac{1}{4} - \frac{p}{12} - \frac{p^2}{105} \right) \gamma^2 - \dots \right] \end{aligned} \quad (6)$$

where the explicit values of ${}_{01}a_1^1$ and ${}_{21}a_1^1$ anticipate the results of further calculation. Only the coefficients ${}_{i1}a_1^1$ need thus be evaluated. It is clear, however, from Peterlin's discussion⁷ that this series for $\langle \mu \rangle_g$ diverges for values of γ greater than 2, i.e., g greater than $4D$. Thus the behavior of particles under high shear gradients cannot be calculated from this series, though as will be shown later, a closed form solution for a spherical particle may be obtained from this approach.

The practical solution of the diffusion equation is based on analogy to Peterlin's treatment⁷ of the hydrodynamic distribution function. Expanding F in powers of p and ϵ

$$F = \sum_{ij} p^i \epsilon^j \Phi_{ij} \quad (7)$$

where Φ_{ij} is similar to F_{ij} in eq 4, with the coefficients ${}_{ij}a_n^m$ and ${}_{ij}b_n^m$ replaced by ${}_{ij}\alpha_n^m$ and ${}_{ij}\beta_n^m$, respectively. Equating coefficients for like powers of p and ϵ

$$\Delta_1 \Phi_{i,j} = \Delta_2 \Phi_{i-1,j} + \Delta_3 \Phi_{i,j-1} \quad (8)$$

where

$$\Delta_1 = \nabla^2 - \gamma \frac{\partial}{\partial \phi}$$

$$\Delta_2 = \gamma \cos 2\phi \frac{\partial}{\partial \phi} + \gamma \cos \theta \sin \theta \sin 2\phi \frac{\partial}{\partial \theta} - 3\gamma \sin^2 \theta \sin 2\phi$$

$$\Delta_3 = -\frac{\sin \phi}{\sin \theta} \frac{\partial}{\partial \phi} + \cos \theta \sin \phi \frac{\partial}{\partial \theta} - 2 \sin \theta \cos \phi$$

The effects of the above operators on a spherical harmonic

$P = P_n^m(\cos \theta) \frac{\cos m\phi}{\sin m\phi}$ are given by

$$\begin{aligned} \Delta_1 P &= -n(n+1) P_n^m(\cos \theta) \frac{\cos m\phi}{\sin m\phi} - \\ &\quad \gamma m P_n^m(\cos \theta) \frac{-\sin m\phi}{\cos m\phi} \end{aligned} \quad (9)$$

$$\begin{aligned} \Delta_2 P &= -\frac{\gamma(n+3)}{2(2n+1)(2n+3)} P_{n+2}^{m+2}(\cos \theta) \frac{\sin(m+2)\phi}{-\cos(m+2)\phi} + \\ &\quad \frac{3\gamma}{2(2n-1)(2n+3)} P_n^{m+2}(\cos \theta) \frac{\sin(m+2)\phi}{-\cos(m+2)\phi} - \\ &\quad \frac{\gamma(n-2)}{2(2n-1)(2n+1)} P_{n-2}^{m+2}(\cos \theta) \frac{\sin(m+2)\phi}{-\cos(m+2)\phi} + \\ &\quad \frac{\gamma(n+3)(n-m+1)(n-m+2)(n-m+3)(n-m+4)}{2(2n+1)(2n+3)} P_{n+2}^{m-2} \times \\ &\quad (\cos \theta) \frac{\sin(m-2)\phi}{-\cos(m-2)\phi} - \frac{3\gamma(n-m+1)(n-m+2)(n+m-1)(n+m)}{2(2n-1)(2n+3)} \times \\ &\quad P_n^{m-2}(\cos \theta) \frac{\sin(m-2)\phi}{-\cos(m-2)\phi} - \\ &\quad \frac{\gamma(n-2)(n+m-3)(n+m-2)(n+m-1)(n+m)}{2(2n-1)(2n+1)} P_{n-2}^{m-2} \times \\ &\quad (\cos \theta) \frac{\sin(m-2)\phi}{-\cos(m-2)\phi} \end{aligned} \quad (10)$$

$$\begin{aligned} \Delta_3 P &= \frac{(n+2)}{2(2n+1)} P_{n+1}^{m+1}(\cos \theta) \frac{\cos(m+1)\phi}{\sin(m+1)\phi} + \\ &\quad \frac{(n-1)}{2(2n+1)} P_{n-1}^{m+1}(\cos \theta) \frac{\cos(m+1)\phi}{\sin(m+1)\phi} - \\ &\quad \frac{(n+2)(n-m+1)(n-m+2)}{2(2n+1)} P_{n+1}^{m-1} \times \\ &\quad (\cos \theta) \frac{\cos(m-1)\phi}{\sin(m-1)\phi} - \\ &\quad \frac{(n-1)(n+m-1)(n+m)}{2(2n+1)} P_{n-1}^{m-1} \times \\ &\quad (\cos \theta) \frac{\cos(m-1)\phi}{\sin(m-1)\phi} \end{aligned} \quad (11)$$

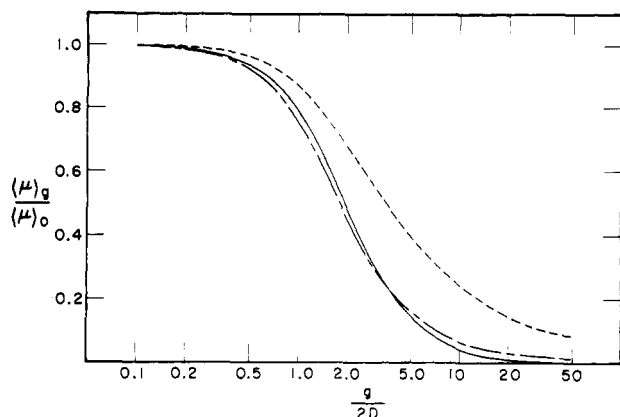


Figure 1. Plots of $\langle \mu \rangle_g / \langle \mu \rangle_0$ as a function of $g/2D$ for spheres (—), rods (···), and disks (---).

From these expressions, recurrence relations may be derived which yield the various coefficients $_{ij}\alpha_n^m$ and $_{ij}\beta_n^m$. The expressions for $_{i0}\alpha_n^m$ and $_{i0}\beta_n^m$ agree with those of Peterlin. In analogy with eq 6, eq 5 and 7 yield

$$\langle \mu \rangle_g = -\frac{\mu\epsilon}{3} \sum_{i=0}^{\infty} i_1 \alpha_i^1 p^i \quad (12)$$

The only coefficients actually required for calculation of the polarization are thus $_{i1}\alpha_1^1$.

Expansion of the distribution function in powers of γ and ϵ permits a closed form solution to be derived for a spherical particle. Moreover, the electric field can in this case be allowed to vary sinusoidally with time.

$$E = E_0 e^{i\omega t} \quad (13)$$

Consideration of the analog of eq 8 for expansion in powers of γ and ϵ gives the recurrence relations

$$2_{01}\alpha_1^1 + \frac{1}{D} \frac{\partial_{01}\alpha_1^1}{\partial t} = -2e^{i\omega t} {}_{00}\alpha_0^0 \quad (14)$$

$$2_{i+1,1}\beta_1^1 + \frac{1}{D} \frac{\partial_{i+1,1}\beta_1^1}{\partial t} = i_1 \alpha_1^1 \quad (15)$$

$$2_{i+1,1}\alpha_1^1 + \frac{1}{D} \frac{\partial_{i+1,1}\alpha_1^1}{\partial t} = -i_1 \beta_1^1 \quad (16)$$

The instantaneous induced polarization $\bar{\mu}_{g\omega}$ may then be calculated from a time-dependent analog of eq 6, as

$$\begin{aligned} \bar{\mu}_{g\omega} &= \frac{\mu^2 E_0}{3kT} \left[\frac{1}{(1 + (i\omega/2D))} - \frac{(\gamma/2)^2}{(1 + (i\omega/2D))^3} + \frac{(\gamma/2)^4}{(1 + (i\omega/2D))^5} + \dots \right] e^{i\omega t} \\ &= \frac{\mu^2 E_0}{3kT} \left[\frac{1 + (i\omega/2D)}{(1 + (i\omega/2D))^2 + (\gamma/2)^2} e^{i\omega t} \right] \quad (17) \end{aligned}$$

The observed polarization is the real part of the above expression or

$$\langle \mu \rangle_{g\omega} = \frac{\mu^2 E_0}{3kT} \times \frac{1 + (\omega/2D)^2 + (g/4D)^2}{[1 + (\omega/2D)^2 + (g/4D)^2]^2 - 4(\omega/2D)^2(g/4D)^2} \times \cos \omega t \quad (18)$$

which, at zero shear, is identical with the Debye formula.

Results and Discussion

Coefficients were evaluated on an IBM 7094-7040 Direct Coupled System using calculational methods similar to

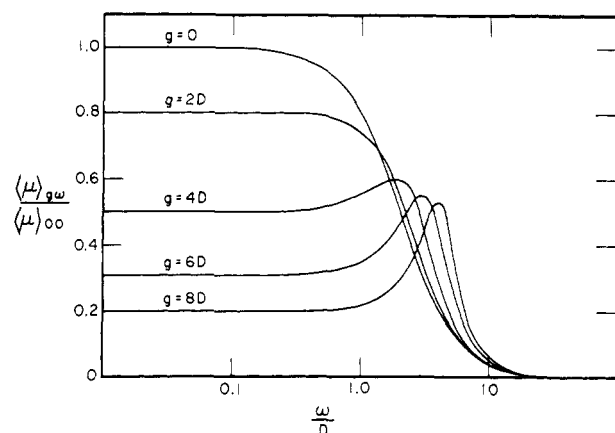


Figure 2. Plot of $\langle \mu \rangle_{g\omega} / \langle \mu \rangle_0$ for a spherical particle as a function of ω/D for various rates of shear.

those developed by Sheraga, *et al.*,⁹ for studies concerning double refraction of flow. A Fortran IV program calculated the distribution function for the zeroth and first power of the electric field up to the 22nd power of p for values of $g/2D$ ranging from 0 to 50. Only values of $_{i1}\alpha_1^1$ were retained. The results of this calculation are expressed as the ratio of the mean dipole moment measured at finite shear to that measured at zero shear

$$\frac{\langle \mu \rangle_g}{\langle \mu \rangle_0} = \frac{\sum_{i=0}^{22} i_1 \alpha_1^1 p^i}{_{01}\alpha_1^1} \quad (19)$$

Since $_{01}\alpha_1^1 = -1$, this expression becomes

$$\frac{\langle \mu \rangle_g}{\langle \mu \rangle_0} = 1 - {}_{11}\alpha_1^1 p - {}_{21}\alpha_1^1 p^2 - {}_{31}\alpha_1^1 p^3 \dots \quad (20)$$

which converges for all $|p| \leq 1$.

Table I shows the ratio $\langle \mu \rangle_g / \langle \mu \rangle_0$ as a function of $g/2D$ for spheres and for prolate and oblate ellipsoids of various axial ratios. Figure 1 shows these data for spheres and for infinitely thin rods and disks plotted *vs.* $g/2D$ on a logarithmic scale. For all shapes of ellipsoids, the static polarization decreases with increasing shear. All values in Table I for $\gamma < 2$, *i.e.*, $g < 4D$, agree with those calculated from expansion of the distribution function in powers of γ and ϵ (eq 6). Further, the results shown for the sphere coincide with those obtained from eq 18. Figure 2 shows the frequency dependence of the polarization of a spherical particle calculated from eq 18 for a variety of shear rates. Of special interest is the maximum in the observed polarization occurring for large shear rates, *i.e.*, $g \geq 4D$, at an electric field frequency ω of approximately $g/2$.

Figure 1 shows that the effect of shearing force on the induced dipole moment due to permanent dipole orientation is, at least for ellipsoids, quite insensitive to molecular shape. The corollary is that measurements of this effect can yield little structural information other than the rotary diffusion constant of the particle in question.

Only for rod-shaped particles are there experimental data which may be compared with theory. In these cases the quantitative agreement of the model with the very limited available data seems quite satisfactory. The clearest demonstration of this agreement comes from an earlier experimental study of the author on the effect of shearing force on the orientation polarization of helical PBLG in an Arochlor 1242¹⁰-tetrachloroethylene mixture. Rotary diffusion constants for the polymers were determined by viscosity measurements, and dielectric data were extrapolated to zero concentration and frequency. Figure 3 shows the data

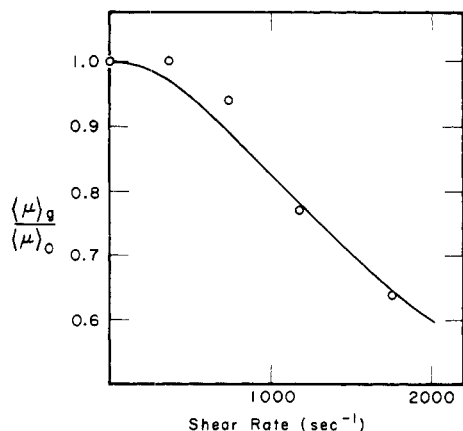


Figure 3. Plot of $\langle \mu \rangle_g / \langle \mu \rangle_0$ as a function of shear rate for 100,000 molecular weight PBLG in Aroclor 1242–tetrachlorethylene (80:20 v/v). The smooth curve represents results of Table I for a rigid rod of rotary diffusion constant equal to that measured for the PBLG.

for 100,000 molecular weight PBLG plotted together with the calculated curve for a rigid rod of equivalent rotary diffusion constant (400 sec⁻¹). PBLG undergoes end-to-end aggregation in this solvent system and hence the observed rotary diffusion constant does not agree with that predicted from the molecular weight and α -helical geometry. It is also clear that these aggregated polymers are not rigid rods in solution. The sample polarization is nonetheless satisfactorily predicted from the observed rotary diffusion con-

stant in spite of the indeterminate conformation of the polymer; this is perhaps explained by the predicted insensitivity of the effect to molecular shape.

No spherical molecules have as yet been examined for the effect, predicted by eq 18, of shearing force on the frequency dependence of their observed polarization. Experimental data for PBLG⁵ indicate, however, that rod-shaped particles exhibit the qualitative features of the effect predicted for spheres. When dielectric constants of PBLG solutions are plotted vs. frequency, the resulting curves show, for sufficiently large shear rates, distinct maxima highly reminiscent of Figure 3.

Acknowledgment. The author wishes to thank Dr. James M. O'Reilly for his valuable advice and encouragement.

References and Notes

- (1) Department of Chemistry, University of Colorado, Boulder, Colo. 80302.
- (2) (a) N. Saito and T. Kato, *J. Phys. Soc. Jap.*, **12**, 1393 (1957); (b) A. Peterlin and C. Reinhold, *Kolloid.-Z. Z. Polym.*, **204**, 23 (1965).
- (3) P. Wendisch, *Kolloid.-Z. Z. Polym.*, **199**, 24 (1964).
- (4) B. Jacobsen and M. Wenner, *Biochim. Biophys. Acta*, **13**, 3604 (1956).
- (5) B. G. Barisas and J. M. O'Reilly, General Electric Company Technical Information Series Report No. 69-C-015, Schenectady, N.Y., 1968.
- (6) S. Takashima, *J. Phys. Chem.*, **74**, 4446 (1970).
- (7) A. Peterlin, *Z. Phys.*, **111**, 232 (1938).
- (8) W. Magnus, F. Oberhettinger, and R. P. Soni, "Formulas and Theories for the Special Functions of Mathematical Physics," Springer-Verlag, New York, N.Y., 1966, p 171.
- (9) H. A. Scheraga, J. T. Edsall, and J. O. Gadd, *J. Chem. Phys.*, **19**, 1101 (1951).
- (10) A Monsanto polychlorinated biphenyl.

Coupling Reactions of Vinylsilanes with Silica and Poly(ethylene-co-propylene)

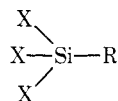
A. N. Gent* and E. C. Hsu

Institute of Polymer Science, The University of Akron, Akron, Ohio 44325.

Received August 26, 1974

Abstract: By means of nir spectroscopy, direct chemical bonding between model silane compounds and finely divided silica particles has been demonstrated. Addition of the silane molecules to silica, catalyzed by *n*-propylamine, is inferred to take place *via* interchange reactions with silanol groups on the silica surface. A maximum addition of about one silane group per 100 Å² of silica surface was attained. When silica treated with vinyl silane in this way was dispersed in poly(ethylene-co-propylene) and a free-radical intermolecular cross-linking reaction was carried out, from 35 to 50% of the vinyl groups disappeared, presumably as a result of radical combinations with polymer molecules. Thus, covalent bonding is deduced to take place between silica and polymer *via* surface silane groups, at a density in the present case of about 0.4 bonds per 100 Å² of interfacial area.

Organofunctional silane coupling agents have been successfully used to improve the adhesion of organic polymers to glass.¹⁻⁴ They usually have the following structure



where X denotes alkoxy (usually methoxy or ethoxy) or halogen (usually chlorine). The X groups hydrolyze in the presence of water to form silanols which in turn can condense with OH groups present on the surface of glass to form direct siloxane bonds. The groups denoted R are usually chosen to be compatible or chemically reactive with the polymers to be bonded.

Theoretically, only one hydrolyzable group is required

per silane molecule. However, it is common to employ coupling agents having two or three per molecule, probably to increase their solubility in water and thus make their application to glass easier, and also to increase their rate of reaction with glass. On the other hand, polyfunctional hydroxysilane molecules can condense with each other to yield linear or branched polysiloxanes, in place of the desired reaction with glass. It seems likely that both of these reactions go on simultaneously, in practice, although firm evidence is lacking. Indeed, although it is generally thought that covalent bonding takes place between glass and coupling agent, and between coupling agent and polymer, no unequivocal proof of these reactions is known to the present authors. A number of observations including infrared transmission and reflection spectroscopy,⁵⁻⁷ Raman spectroscopy,⁸ and ellipsometry^{7,9} have indicated that chemical bonding to